[1]Institute of Linguistics, Shanghai International Studies University, 1550 Wenxiang Road, Shanghai 201620, China,
[2]Beijing Key Laboratory of Behavior and Mental Health, School of Psychological and Cognitive Sciences, Peking University, 5 Yiheyuan Road, Beijing 100871, China,
[3]Institute of Psychology and Bc [nioioraioioryu.3461 Tm .0557.6(eking)S6(201620,)-238.J 0 I4/Shanghai Key Laboratory of Psychotic Disorders, Shanghai Mental Health Center, Sh
Shanghai 200030, China

,

[5]Shanghai Center for Brain Science and Brain-Inspired Intelligence Technology, 555 Qiangye Road Shanghai 200125, China,
[6]Beijing Neurosurgical Institute, Capital Medical University, 119 South Fourth Ring West Road, Beijing 100070, China,
[7]Peking-Tsinghua Center for Life Sciences, Peking University, 5 Yiheyuan Road, Beijing 100871, China,
[8]

recommendation letter for my student" as a reply to the question "What did you do this morning?", the speaker simply describes the situation, and hence the attitude of the interlocutors toward the task in the reply is not clear.

While linguistic communications are regarded as goal-directed actions with different functions by linguistic theories, it is barely known how these communicative functions are represented in the brain. One straightforward prediction is that communicative functions are represented in brain areas that subserve action programing or preparation. Consistent with this prediction, the co-evolution of humans' linguistic ability and motor skills (e.g. tool use) has been highlighted from neurophysiological, neurocognitive, and anthropological perspectives (Rizzolatti and Arbib 1998; Arbib 2011; Stout and Chaminade 2012; Pulvermüller 2018; Thibault et al. 2021). As a demonstration, linguistic communications between tutors and learners can improve the efficiency of learning to make Paleolithic tools (Morgan et al. 2015), and the activation in the premotor region of the human brain increases with the evolutionary progress of Paleolithic tool-making skills (Stout et al. 2008). Moreover, contributions of the premotor region to communications through language or language-like manners are revealed not only in humans (Hauk et al. 2004; Wilson et al. 2004; Egorova et al. 2016; Dreyer and Pulvermüller 2018), but also in species including avian (Thompson et al. 2011), Cercopithecinae (Gil-da-Costa et al. 2006), and *Pan*

Table 1. English translation of the scripts in the fMRI study, with original Chinese version of critical sentences.

Communicative function	Context	Pre-critical sentence	Critical sentence
Promise	The sales department conducted a survey, and Xiaoli was assigned to analyze the survey data this week. But Xiaoli was too busy to analyze it because he had		

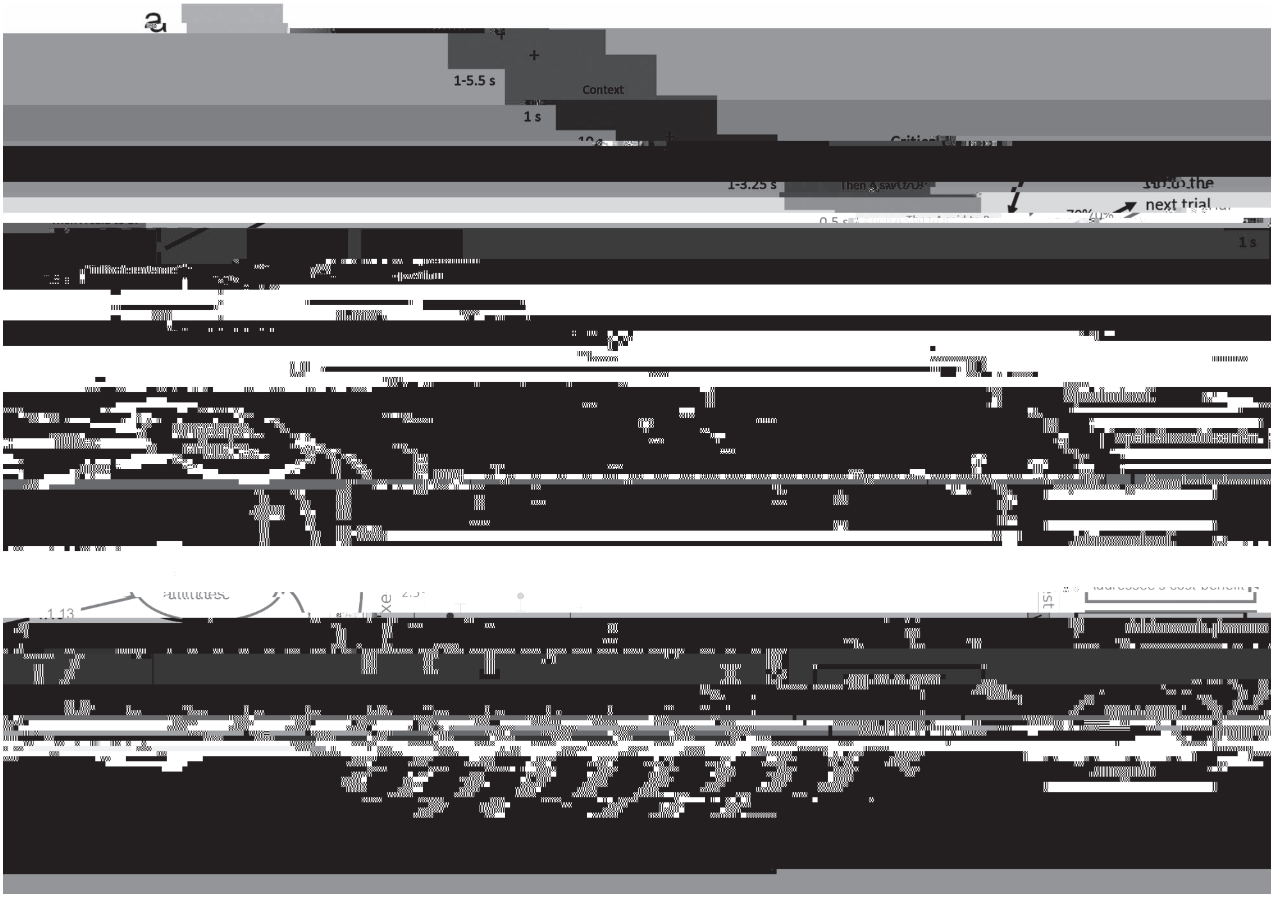

Fig. 1. Experimental procedure and behavioral results of the fMRI study. a) In each trial, the context, the pre-critical sentence, and the critical sentence were presented sequentially in written form. The critical sentence is enclosed by the dashed rectangle (not shown in the actual experiment). In 24 catch trials (30% of all trials), participants were instructed to respond to a comprehension question. b) Results of Bayesian logistic mixed modeling. The posterior estimates of the fixed effects (vertical axis) for rating features (horizontal axis) in the "*Promise* vs. *Reply-1*" model (upper panel, black) and the "*Request* vs. *Reply-2*" model (lower panel, gray) are illustrated. The solid dots represent mean posterior estimates, the error bars represent 95% CrIs. A 95% CrI excluding 0 indicates a statistically significant predictability of the corresponding feature. c) The 3-factor model of the CFA. The ellipses represent the accounting factors and the rectangles represent the rating features. The correlations between the accounting factors and the loadings of the accounting factors on the features are embedded in the arrows.

a gray background (RGB: 180, 180, 180). In each trial (Fig. 1a), a fixation cross was firstly presented at the center of the screen for a jitter duration of 1–5.5 s, followed by a cross presented at the upper left part of the screen where the first character of the context would located. This fixation was presented for 1 s to direct participants' attention. The context was presented for 10 s and followed by a cross presented at the center for another jitter duration of 1–3.25 s. A cross was then presented for 1 s at the upper left part of the screen where the first character of the pre-critical sentence was located. After the offset of the cross, the pre-critical sentence was presented. After the pre-critical sentence had been presented for 1 s, a cross was presented below the pre-critical sentence, where the first character of the critical sentence would be located. This cross lasted for 0.5 s together with the pre-critical sentence. After the offset of the cross, the critical sentence was presented within double quotes for 4 s, together with the pre-critical sentence. To engage the participants into reading the script, a comprehension question, which was related to the information of both the contexts and the critical sentences, was added to each of the 24 catch trials (30% of all trials, each condition had 6 catch trials). At the end of these catch trials, a triangle was presented at the center for a jitter duration of 1–6.6 s, followed by a comprehension question. Participants were instructed to make "yes" or "no" response by pressing the button on the response box in their left or right hand. Half of the participants were instructed to press the left button for "yes" and the right button for "no," and the other half made their responses with a reversed button-hand assignment. Half of these trials required a "yes" as correct response and the other half required a "no" as correct response. Prior to the scanning, participants performed 10 practice trials with scripts not in the experimental lists.

Poel

(the speaker/addressee would be benefitted highly if the task has been accomplished); (6) speaker's pleasure and (7) addressee's pleasure, from 1 (the speaker/addressee is very unpleased when communicating) to 7 (the speaker/addressee is very pleased when communicating); (8) relative power, from 1 (the addressee's power is definitely higher than the speaker's) to 7 (the speaker's power is definitely higher than the addressee's); (9) the social distance between the interlocutors, from 1 (very close) to 7 (very remote); and (10) mitigation of the critical sentence, from 1 (not mitigated at all) to 7 (highly mitigated).

Statistical analysis of post-scanning ratings

Bayesian logistic mixed models

To assess the extent to which communicative functions could be predicted by the 10 features, the post-scanning ratings were fitted with Bayesian logistic mixed models using the *brms* package (Bürkner 2017) in R environment. The 2 pair-wise predictions, "*Promise* vs. *Reply-1*" and "*Request* vs. *Reply-2*", were assessed respectively with an independent model. In each model, the response variable was the communicative function, the predictors were the ratings of the 10 features. Full models were fitted to reduce type-I error rate (Barr et al. 2013). The priors for all fixed slopes and the fixed intercept were *Normal*(0,100), while the priors for standard deviations were *Cauchy*(0,5). Within the variance–covariance matrices of the by-participant and by-item random effects, priors were defined for the correlation matrices using a Lewandowski-Kurowicka-Joe (LKJ) prior with parameter η 1.0 (Lewandowski et al. 2009

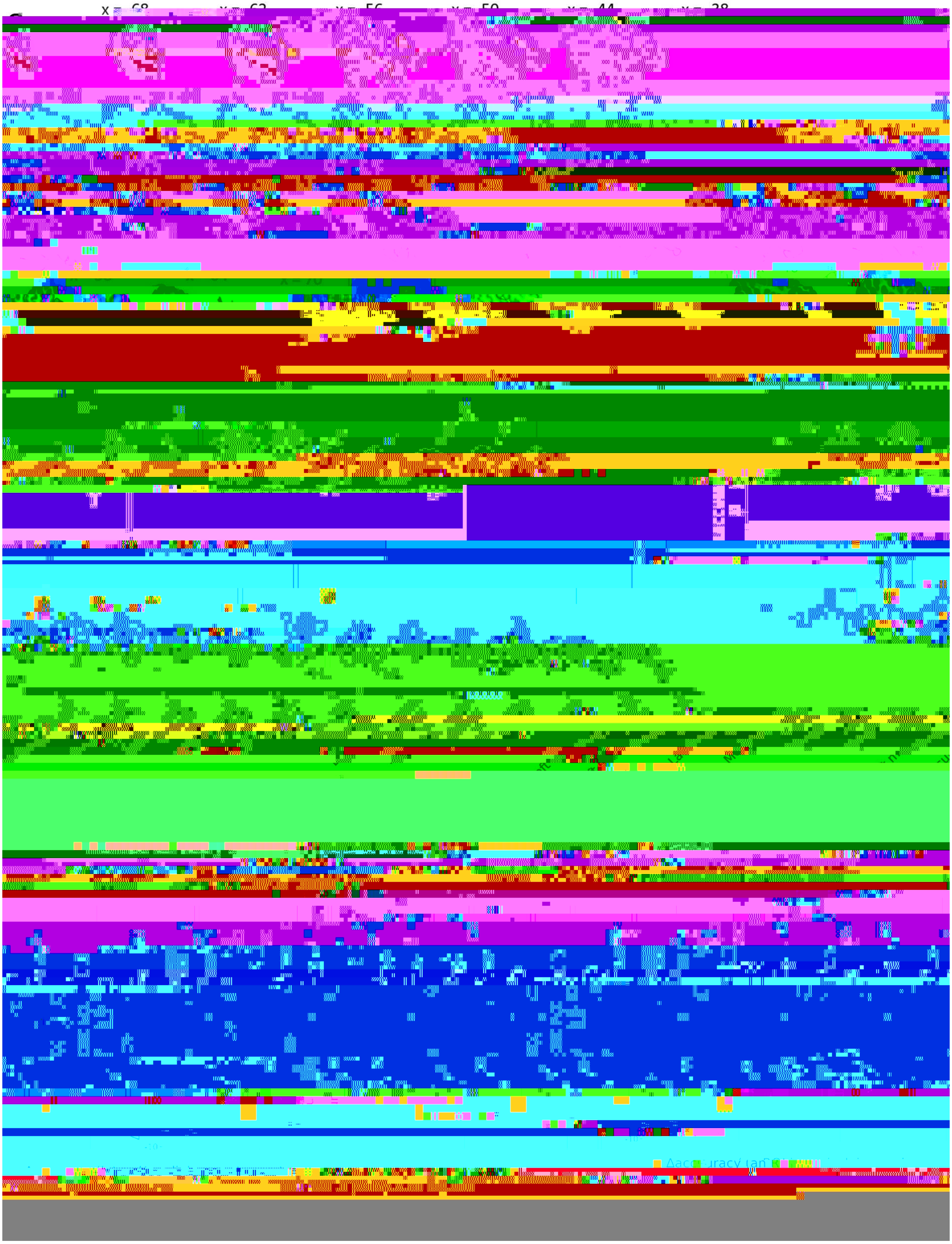

Fig. 2. MVPC results of fMRI data. a) Five ROIs were defined. Red, LPMC; pink, MPMC; blue, Broca's area (BA44); yellow, Broca's area (BA45); green, LMTG; orange, LSTG (x-coordinates based on the MNI system). b) Results of ROI-based MVPCs. The classification accuracies (vertical axis) in the ROIs (horizontal axis) for the 4 pair-wise classifications are illustrated. Left top, *Promise* vs. *Reply-1*; right top, *Request* vs. *Reply-2*; left bottom, *Promise* vs. *Request*; right bottom, *Reply-1* vs. *Reply-2*. The red dashed lines represent the chance-level percentage of binary classification (50%). Red stars represent statistical significance of permutation tests with Bonferroni correction. c) Results of combinatorial MVPCs. Left panel, *Promise* vs. *Reply-1*; right panel, *Request* vs. *Reply-2*. Vertical axes illustrate the improvement in classification accuracy contributed by an added ROI for an initial ROI. Red stars represent statistical significance of permutation tests with Bonferroni correction. Each yellow dot indicates the improvement in classification accuracy contributed by a premotor ROI for a perisylvian ROI. Each blue dot indicates the improvement in classification accuracy contributed by a perisylvian ROI for a premotor ROI. Each black dot indicates the difference between the improvement in classification accuracy contributed by a premotor ROI for a perisylvian ROI and that contributed by a perisylvian ROI for a premotor ROI. The crowded small gray dots indicate data points of null distributions for permutation tests.

OI-ba ed m l i aria e pa ern cla ifi a ion

To detect differences in activity patterns representing the different communicative functions, multivariate pattern classification (MVPC) was conducted for each ROI using the *PyMVPA* toolbox (Hanke et al. 2009). In each ROI, the voxel-level parameter estimates of the critical sentences were extracted, detrended along time series, and transformed into *Z*-scores across runs. For each ROI, cross-validated classifications of communicative functions were performed using a linear support vector machine (SVM) as a classifier. Four pair-wise classifications were performed: (1) *Promise* vs. *Reply-1*; (2) *Request* vs. *Reply-2*; (3) *Promise* vs. *Request*; (4) *Reply-1* vs. *Reply-2*. For each pair-wise classification, a participant-based cross-validation with 50 repetitions were conducted. Each repetition consisted of a training set of data from 45 (approximately 80% of all data) randomly selected participants and a test set of data from the remaining 11 participants (approximately 20% of all data). For each repetition, a cross-validated accuracy was computed as a percentage of correct classifications of the test set to evaluate the performance of a classifier, and the mean accuracy averaged over the 50 repetitions was calculated.

Statistical significance of the classification accuracy was tested using permutation-based classifications with 2,000 repetitions for each pair-wise classification (Stelzer et al. 2013). In each repetition, the participant-based cross-validation procedure described above was performed on the data with permuted communicative functions, generating 2,000 null cross-validated accuracies derived for each pair-wise classification. Probabilities (*P*-values) of the observed accuracies against the distribution of the permutation-based null accuracies were computed. Statistical significance was determined by a Bonferroni-corrected significance threshold of $P < 0.002$ (24 comparisons were conducted in total). A significant accuracy indicates that the multivariate activity in an ROI showed distinct patterns between the pair-wise communicative functions, leading to an inference that the ROI represents the information on these functions, but the accuracy

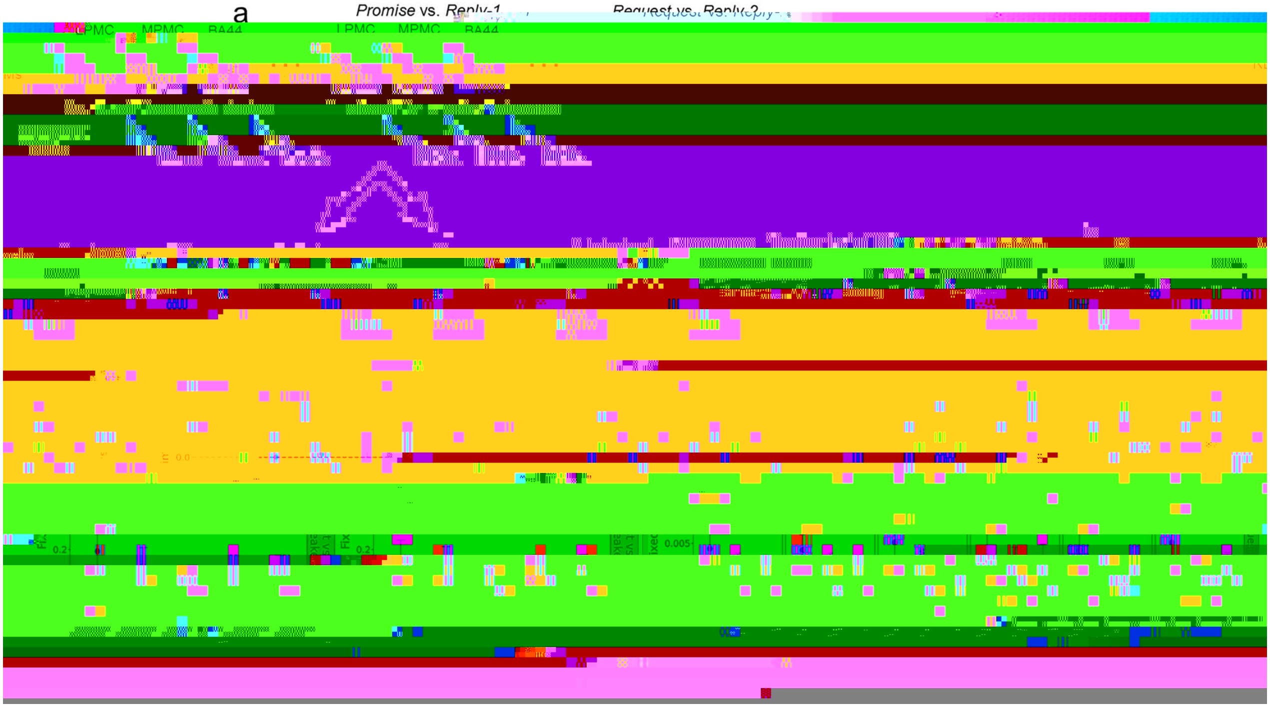

Fig. 3. RSAs of fMRI data. a) The brain RDMs and the behavioral RDMs for the 2 pair-wise predictions, "*Promise* vs. *Reply-1*" and "*Request* vs. *Reply-2*". b) The equation of the RS encoding model, which includes a brain RDM as response variable and the 3 behavioral RDMs as predictors (see Methods for details). c) Results of RS encoding models. d) The equation of the RS decoding model, which includes a behavioral RDM as response variable, 5 brain RDMs as predictors, and the other 2 behavioral RDMs as covariates (see *Methods* for details). e) Left panel, results of RS decoding models with the LPMC RDM and the RDMs of the prerisylvian ROIs as predictors; right panel, results of RS decoding models with the MPMC RDM and the RDMs of the perisylvian ROIs as predictors. For a, b, and d, the lower-triangular RDMs from one participant are shown as examples (only for illustrative purpose). For c and e, the posterior estimates (vertical axis) of the "*Promise* vs. *Reply-1*" models (upper panel, red) and the "*Request* vs. *Reply-2*" models (lower panel, turquoise) are illustrated. The solid dots represent mean posterior estimates, the error bars represent Bonferroni corrected CrIs (99.86% CrI for the encoding models and 99.92% CrI for the decoding models). The dashed gray lines indicate 0 for fixed effect estimates. An effect was determined as significant when the Bonferroni-corrected CrI excluded 0.

RDM), the variance of the addressee's attitudes (Addressee RDM), and the variance of the contextual information (Context RDM), respectively. For each behavioral factor, the ratings of the 3 dimensions for each trial were represented in a 3-dimensional space, and the Euclidian distance between each 2 rating points was calculated as the value in each cell of the behavioral RDM. Each of the 3 behavioral RDM also had a 40 (2 conditions 20 trials per condition) 40 structure.

For each ROI and each of the 2 pair-wise predictions, a representational similarity (RS) encoding model was used to assess the extent to which the brain RDM can be predicted by the behavioral RDMs (Fig. 3b). Specifically, a Bayesian linear mixed model was conducted with Eq. (

brain RDM of a specific ROI, the RS decoding model estimated the coefficients of the brain RDMs of different ROIs in predicting a specific behavioral RDM. An effect was tested with Bonferroni corrected CrIs, 99.86% CrI for the encoding models where 24 (6 brain RDMs 3 behavioral RDMs 2 pair-wise predictions) effect estimates were tested, and 99.92% CrI for the decoding models where 60 (3 behavioral RDMs 5 brain RDMs 2 models with different premotor ROIs 2 pair-wise predictions) effect estimates were tested. An effect was determined as significant when Bonferroni corrected CrI excluded 0.

Study 2: lesion study

Par ipan

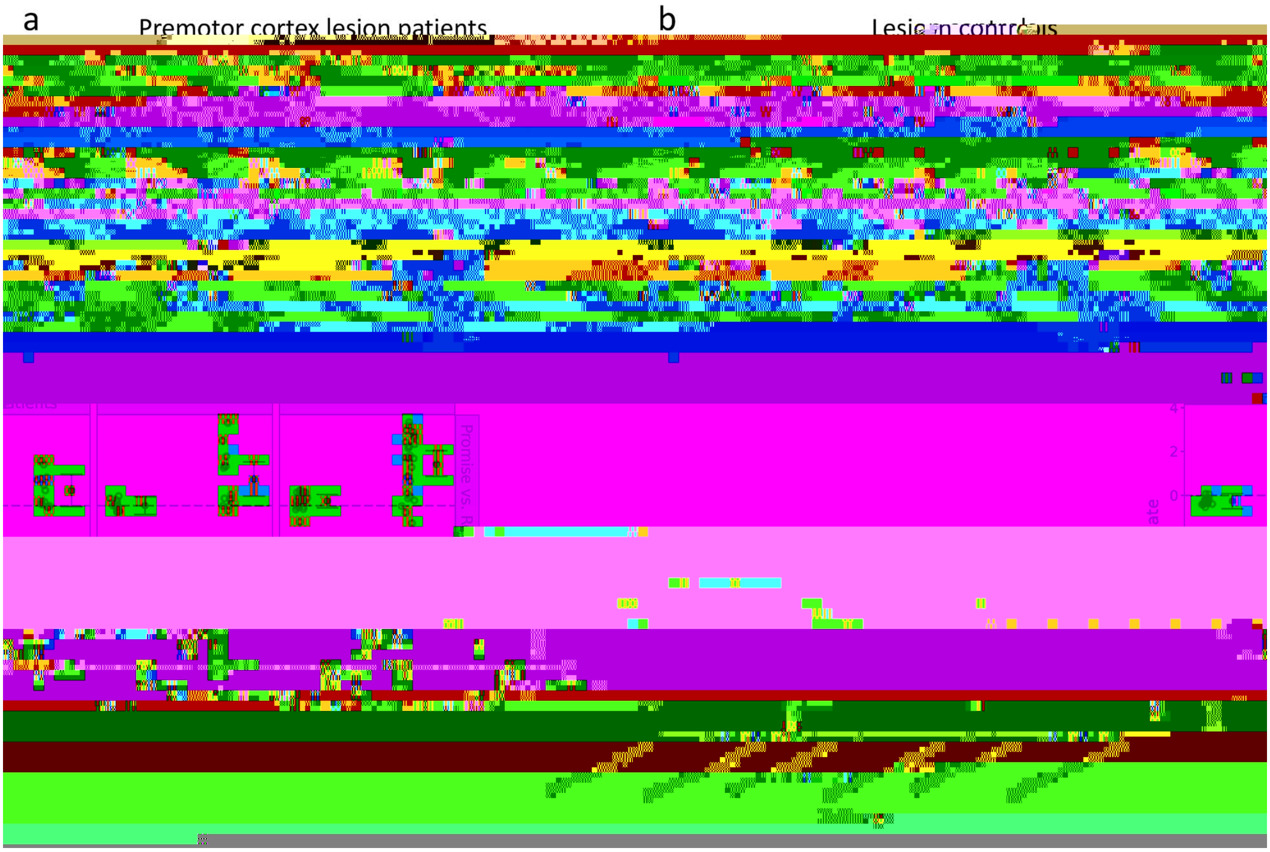

Fig. 4. Results of the lesion study. Lesion reconstructions for a) premotor cortex lesion patients and b) lesion controls. The text in black indicates the
x

Table 2. MVPC results of fMRI data.

ROI-based MVPCs

ROI (n voxels)	Index	Pair-wise classification: *Promise* vs. *Reply-1*	*Request* vs. *Reply-2*	*Promise* vs. *Request*	*Reply-1* vs. *Reply-2*
LPMC (5507)	Accuracy (%)	60	67	55	50
	P	<0.0005	<0.0005	<0.0005	0.534
MPMC (5227)	Accuracy (%)	64	67	58	58
	P	<0.0005	<0.0005	<0.0005	<0.0005
Left BA44 (1443)	Accuracy (%)	56	58	55	51
	P	<0.0005	<0.0005	<0.0005	0.128
Left BA45 (979)	Accuracy (%)	53	58	58	49
	P	<0.0005	<0.0005	<0.0005	0.827
LMTG (1760)	Accuracy (%)	61	60	55	51
	P	<0.0005	<0.0005	<0.0005	0.078
LSTG (1147)	Accuracy (%)	56	57	51	51
	P	<0.0005	<0.0005	0.018	0.028

Combinatorial MVPCs of Δaccuracy (initial ROI, added ROI)

Pair-wise classification	Premotor ROI	Perisylvian ROI	Δaccuracy (perisylvian ROI, premotor ROI) Δaccuracy (%)	P	Δaccuracy (premotor ROI, perisylvian ROI) Δaccuracy (%)	P	Difference between Δaccuracies Δaccuracy (%)	P
Promise vs. *Reply-1*	LPMC	Left BA44	18	<0.0005	8	<0.0005	10	<0.0005
		Left BA45	21	<0.0005	5	<0.0005	16	<0.0005
		LMTG	4	0.0015	5	<0.0005	1	0.5
		LSTG	13	<0.0005	4	0.0045	9	<0.0005
	MPMC	Left BA44	22	<0.0005	5	<0.0005	17	<0.0005
		Left BA45	26	<0.0005	4	0.001	22	<0.0005
		LMTG	10	<0.0005	5	<0.0005	5	<0.0005
		LSTG	17	<0.0005	1	0.1565	16	<0.0005
Request vs. *Reply-2*	LPMC	Left BA44	17	<0.0005	4	0.002	12	<0.0005
		Left BA45	15	<0.0005	3	0.0115	12	<0.0005
		LMTG	13	<0.0005	3	0.0055	10	<0.0005
		LSTG	16	<0.0005	2	0.0725	14	<0.0005
	MPMC	Left BA44	17	<0.0005	5	<0.0005	12	<0.0005
		Left BA45	15	<0.0005	4	0.0015	11	<0.0005
		LMTG	14	<0.0005	5	<0.0005	9	<0.0005
		LSTG	16	<0.0005	3	0.01	13	<0.0005

Texts in bold indicate statistical significance for the permutation-based significance testing with Bonferroni correction. For ROI-based MVPCs, accuracies were tested with Bonferroni corrected significance threshold of $P < 0.002$. For combinatorial MVPCs, statistical significances for the permutation tests at the first step and the second step were determined b560.00053

Table 3. RSA results of fMRI data.

Representational similarity encoding model							
		Behavioral RDM					
		Speaker		Addressee		Context	
ROI	Prediction	*b*	99.86% CrI	*b*	99.86% CrI	*b*	99.86% CrI
LPMC	*Promise* vs. *Reply-1*	0.001	[0.003, 0.001]	0.007	[0.004, 0.01]	0.0003	[0.002, 0.003]
	Request vs. *Reply-2*	0.004	[0.002, 0.007]	0.001	[0.001, 0.004]	0.001	[0.002, 0.003]
MPMC	*Promise* vs. *Reply-1*	0.001	[0.003, 0.002]	0.007	[0.004, 0.01]	0.0003	[0.003, 0.003]
	Request vs. *Reply-2*	0.004	[0.002, 0.006]	0.001	[0.002, 0.004]	0.001	[0.002, 0.003]

Supplementary material

Supplementary material is available at *Cerebral Cortex* online.

Funding

This work was sponsored by the China Postdoctoral Science Foundation (2021M702211, awarded to WC), the Shanghai Sailing Program (20YF1422100, awarded to LW), the National Science Foundation of China (32000779, awarded to LW), the National Natural Science Foundation of China (81729001, awarded to ZG), and the National Science Foundation of China (31630034, 71942001, awarded to XZ).

Conflict of interest statement: The authors declare no conflict of interest.

References

Amunts K, Schleicher A, Bürgel U, Mohlberg H, Uylings HBM, Zilles K. Broca's region revisited: cytoarchitecture and intersubject variability. *J Comp Neurol*. 1999:412:319–341.

Andraszewicz S, Scheibehenne B, Rieskamp J, Grasman R, Verhagen J, Wagenmakers E-J. An introduction to Bayesian hypothesis testing for management research. *J Manag*. 2015:41:521–543.

Arbib MA. From mirror neurons to complex imitation in the evolution of language and tool use. *Annu Rev Anthropol*. 2011:40: 257–273.

Arbib MA. Towards a computational comparative neuroprimatology: framing the language-ready brain. *Phys Life Rev*. 2016:16:1–54.

Arnold K, Zuberbühler K. Semantic combinations in primate calls. *Nature*. 2006:441:303–303.

Austin JL. *How to do things with words*. Cambrige, MA: Harvard University Press; 1975.

Avenanti A, Bolognini N, Maravita A, Aglioti SM. Somatic and motor components of action simulation. *Curr Biol*. 2007:17: 2129–2135.

Aziz-Zadeh L, Koski L, Zaidel E, Mazziotta J, Iacoboni M. Lateralization of the human mirror neuron system. *J Neurosci*. 2006:26: 2964–2970.

Garrod S, Pickering MJ. Why is conversation so easy? *Trends Cogn Sci*. 2004:8:8–11.

Gelman A, Rubin DB. Inference from iterative simulation using multiple sequences. *Stat Sci*. 1992:7:457–472.

Geyer S. *The microstructural border between the motor and the cognitive domain in the human cerebral cortex*. Berlin, Heidelberg: Springer; 2004

Gil-da-Costa R, Martin A, Lopes MA, Muñoz M, Fritz JB, Braun AR. Species-specific calls activate homologs of Broca’s and Wernicke’s areas in the macaque. *Nat Neurosci*. 2006:9:1064–1070.

Gordon RM. The simulation theory: objections and misconceptions. *Mind Lang*. 1992:7:11–34.

Shibata M, Abe J-i, Itoh H, Shimada K, Umeda S. Neural processing associated with comprehension of an indirect reply during a scenario reading task. *Neuropsychologia*. 2011:49: 3542–3550.

Smith SM. Fast robust automated brain extraction. *Hum Brain Mapp*. 2002:17:143–155.

Stelzer J, Chen Y, Turner R. Statistical inference and multiple testing correction in classification-based multi-voxel pattern analysis (MVPA): random permutations and cluster size control. *NeuroImage*. 2013:65:69–82.